Since January 2020 Elsevier has created a COVID-19 resource centre with free information in English and Mandarin on the novel coronavirus COVID-19. The COVID-19 resource centre is hosted on Elsevier Connect, the company's public news and information website.

Review

Monomeric Intermediates Formed by Vesiculovirus Glycoprotein during Its Low-pH-induced Structural Transition

Abbas Abou-Hamdan, Laura Belot, Aurélie Albertini and Yves Gaudin

Institute for Integrative Biology of the Cell (I2BC), *CEA, CNRS, Univ. Paris-Sud, Université Paris-Saclay, 91198 Gif-sur-Yvette cedex, France*

Correspondence to Yves Gaudin: *yves.gaudin@i2bc.paris-saclay.fr*
https://doi.org/10.1016/j.jmb.2018.04.015
Edited by P-Y Lozach

Abstract

Vesiculoviruses enter cells by membrane fusion, driven by a large, low-pH-induced, conformational change in the fusion glycoprotein (G) that involves transition from a trimeric pre-fusion to a trimeric post-fusion state. G is the model of class III fusion glycoproteins which also includes the fusion glycoproteins of herpesviruses (gB) and baculoviruses (gp64). Class III fusion proteins combine features of the previously characterized class I and class II fusion proteins. In this review, we first present and discuss the data that indicate that the Vesiculovirus G structural transition proceeds through monomeric intermediates. Then, we focus on a recently determined crystal structure of the Chandipura virus G ectodomain that contained two monomeric intermediate conformations of the glycoprotein, revealing the chronological order of the structural changes in the protein and offering a detailed pathway for the conformational change, in agreement with electron microscopy data. In the crystal, the intermediates were associated through their fusion domain in an antiparallel manner to form an intermolecular β-sheet. Mutagenesis indicated that this interface is functionally relevant. All those structural data challenge the current model proposed for viral membrane fusion. Therefore, we wonder if this mode of operating is specific to Vesiculovirus G and discuss data indicating that class II fusion glycoproteins are monomeric when they interact with the target membrane but also crystal structures suggesting the existence of non-trimeric intermediates for influenza hemagglutinin which is the prototype of class I fusion proteins.

Introduction

The Vesiculovirus genus is one of the six genera of the rhabdovirus family. The prototype vesiculovirus is vesicular stomatitis virus (VSV). It is an arbovirus that can infect insects, cattle, horses and pigs. In mammals, its ability to preferentially infect and kill tumor cells makes it a promising oncolytic virus for the treatment of cancer [1–3]. Although VSV-associated disease is generally benign, other vesiculoviruses can be deadly to humans. This is the case for the Chandipura virus (CHAV), which is an emerging human pathogen associated with deadly encephalitis, principally affecting children in the tropical areas of India and which has, in recent years, caused several outbreaks with high mortality rates [4].

As all rhabdoviruses, vesiculoviruses are enveloped viruses having a rigid bullet shape with a flat base and a round tip. Their genome encodes five structural proteins including a single transmembrane glycoprotein (G). G is a type I membrane glycoprotein. After cleavage of the amino-terminal signal peptide, the mature glycoprotein is about 500 amino acids long (495 for VSV G). The bulk of the mass of G is located outside the viral membrane and constitutes the amino-terminal ectodomain. G is anchored in the membrane by a single α-helical transmembrane segment. The small intraviral domain is probably involved in interactions with internal proteins. G plays a critical role during the initial steps of virus infection [5]. First, it is responsible for virus attachment to specific receptors, which, in the case of VSV G, are the members of the low-density lipoprotein receptor family [6,7]. After binding, virions enter the cell by a clathrin-mediated endocytic pathway [8,9]. In the acidic environment of the endocytic vesicle, G triggers the fusion between

the viral and endosomal membranes, which releases the genome in the cytosol for the subsequent steps of infection [5]. Fusion is catalyzed by a low-pH-induced large structural transition from a pre- to a post-fusion conformation which are both trimeric [10]. Remarkably, for rhabdoviruses, the structural transition is reversible [11–14], and in fact, there is an equilibrium between different states of G, which is shifted toward the trimeric post-fusion conformation at low pH [5,15].

VSV G structure reveals an organization distinct from both class I fusion glycoproteins, such as the influenza virus hemagglutinin (HA) and the paramyxovirus fusion protein (F), and class II fusion glycoproteins of several positive strand RNA viruses, such as the E protein of flaviviruses and E1 of alphaviruses, and of the bunyaviridae family [16]. In fact, together with baculovirus gp64 [17], herpesviruses gB [18–21] and thogotovirus Gp [22], rhabdovirus G defines the class III of fusion proteins [23]. VSV G is the only member of this class for which high-resolution structures of both the pre- and post-fusion states are available [24,25]. Low-resolution electron microscopy (EM) structures of the putative pre-fusion state of HSV1 gB have been obtained [26,27], but those structures have led to opposite interpretations concerning the orientation of the fusion domains (FDs) either pointing away or toward the anchoring membrane. Nevertheless, the localization of monoclonal antibodies binding sites [26] and spectroscopic characterization of functional fluorescent gB [28] are consistent with a model of pre-fusion gB similar to the pre-fusion VSV G crystal structure [25] (i.e., with the fusion loops pointing toward the anchoring membrane).

Similar to other class III proteins, the polypeptide chain of the G ectodomain folds into three distinct domains termed the FD, the pleckstrin homology domain (PHD) and the trimerization domain (TrD) [23] (Fig. 1). The FD is an extended β-sheet structure at the tip of which are located the two hydrophobic fusion loops that interact with the target membrane to initiate the fusion process. This organization of the class III FD is reminiscent of that of class II fusion proteins. The TrD comprises an α-helix involved in the trimerization of the glycoprotein and a β-sheet-rich region connected to the C-terminal segment of the ectodomain.

During the structural transition, the FD, the PHD and the TrD retain their tertiary structure. Nevertheless, they undergo large rearrangements in their relative orientation due to secondary changes in hinge segments (R1 to R5) which refold during the low-pH induced conformational change. Particularly, in the post-fusion state, the core of the trimer is made by the three TrD central helices (extended by the refolding of segment R4) whose grooves accommodate three lateral helices resulting in the refolding of R5 (Fig. 1). This six-helix bundle organization is very similar to that of the trimeric core of the post-fusion state of some class I fusion glycoproteins such as HIV-1 gp41 or Ebola gp2 [29,30].

In this review, we will present the recent crystalline structures of monomeric intermediates [31] obtained for CHAV G ectodomain and how they fit with numerous historical articles showing the existence of G monomers. We will also discuss the ability of G monomers to form flat antiparallel dimers and the experimental data indicating that those dimers play a role during the fusion process [31]. Finally, we will discuss if this mode of operating is specific to Vesiculovirus glycoproteins. Particularly, we will review EM data indicating that the initial interaction between class II fusion glycoproteins and the target membrane is mediated by monomers and examine some non-trimeric structures of influenza hemagglutinin present in the Protein Data Bank (PDB) but whose oligomerization state and protomer conformation have never been discussed thoroughly before.

Monomeric states of VSV G

The first attempt to characterize the oligomeric status of VSV G revealed that a soluble ectodomain obtained by treatment of virions with cathepsin D is monomeric at high pH [32]. Later, it was shown that G solubilized from membranes with detergent behaves as a monomer at high pH whereas it forms a stable trimer at low pH [11]. In addition, the existence of a thermodynamic equilibrium between monomers and trimers of VSV G solubilized by octylglucoside was demonstrated [33]. This equilibrium was also demonstrated to exist *in vivo* [34,35]. From those pioneering works, it was clear that VSV G trimer was much less stable than HA trimer, which was the best characterized viral fusion glycoprotein at that time [36].

The behavior of VSV G_{th} (residues 1–422, generated by thermolysin-limited proteolysis of viral particles in solution, which has been crystallized) was further characterized using several biophysical techniques, including analytical ultracentrifugation, circular dichroism, EM and small angle X-ray scattering. While the post-fusion trimer was the major species detected at low pH, the pre-fusion trimer was never detected in solution. Indeed, at high pH, G_{th} appeared to be a flexible monomer exploring a large conformational space and adopting more elongated conformations when pH decreases [37].

The oligomeric status of VSV G has also been analyzed at the surface of the viral particle by EM and tomography. Below pH 6, the only structure which is observed is the trimeric post-fusion state which has a tendency to reorganize into regular arrays [38]. Above pH 7, although few pre-fusion trimers are observed [38], the vast majority seems to be flexible monomers

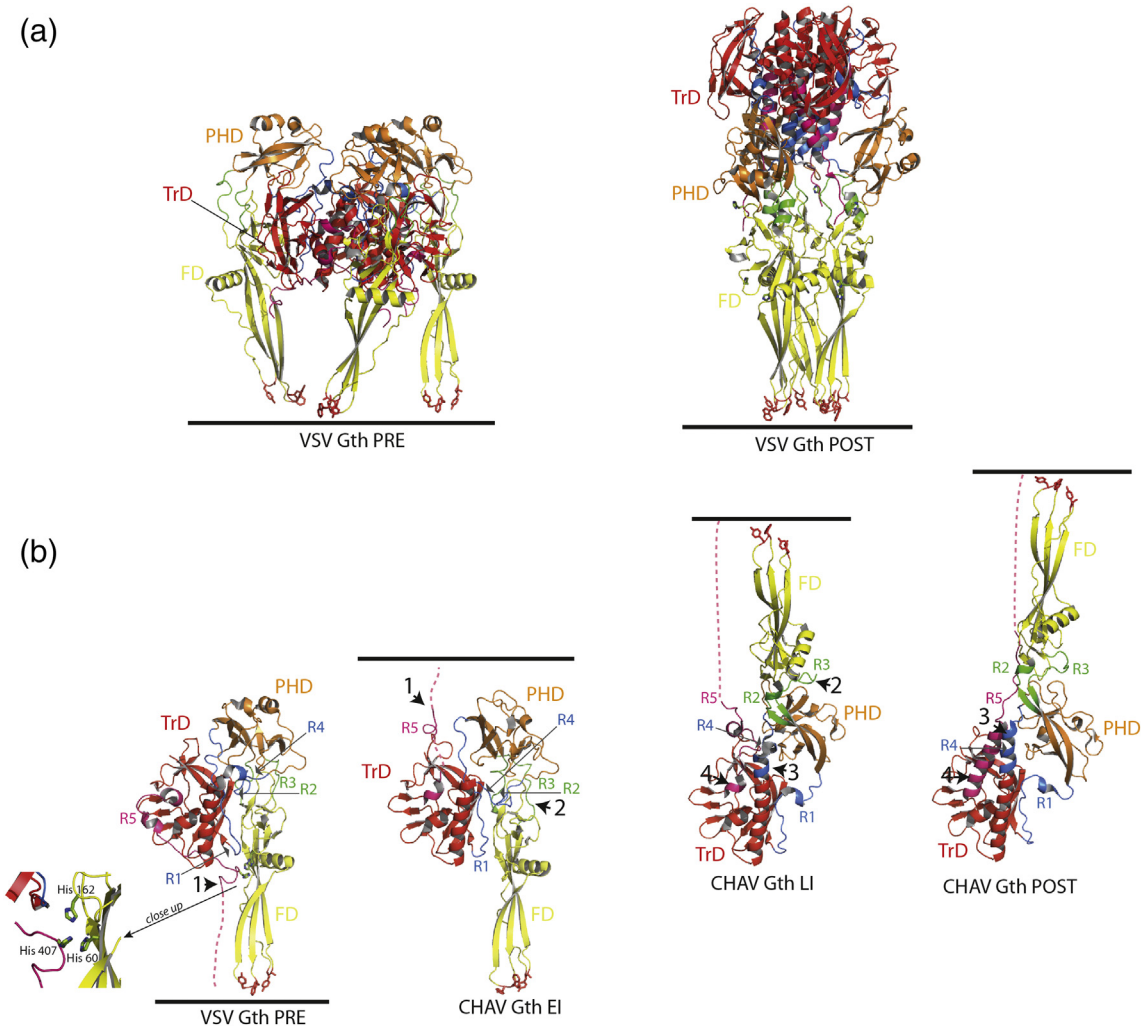

Fig. 1. Structure of vesiculovirus glycoprotein G. (a) Overall structures of the trimeric pre- and post-fusion forms of VSV glycoprotein. Left part: Ribbon diagram of VSV G_{th} pre-fusion trimer (PDB code: 5I2S). Right part: Ribbon diagram of VSV G_{th} post-fusion trimer (PDB code: 5I2M). (b) From left to right: Overall structures of VSV G_{th} pre-fusion protomer, CHAV G_{th} EI (PDB code: 5MDM), CHAV G_{th} LI (PDB code: 5MDM) and CHAV G_{th} post-fusion protomer (PDB code: 4D6W). The major difference between the pre-fusion protomer and the EI is the movement of R5 (arrowhead 1). Then, the refolding of the hinge regions R2 and R3 between PHD and FD (arrowhead 2) together with the partial elongation of the central helix implying R4 allows for the transition to the LI state. At this stage, G is already in a hairpin conformation. The formation of the last amino-terminal turn of the central helix (arrowhead 3) and the refolding of R5 into the lateral helix (arrowhead 4) concomitantly with the final trimerization form the six-helix bundle organization and achieve the structural transition. All the structures are aligned on their TrD. The histidines of the cluster H60, H162 and H407 in the pre-fusion protomer are depicted in green sticks. A close-up view of the cluster is also represented. Color code: TrD is in red, PHD is in orange, FD is in yellow, segments R1 and R4 (indicated by thin gray arrows) are in blue, segments R2 and R3 are in green, and segment R5 and C-terminal segment (cter) are in pink. The residues in the fusion loops at the tip of the FD are in red sticks. The C-terminal segments which are linked to the transmembrane domain are depicted in dashed lines. The position of the membrane relative to the protein is indicated by a black line.

[37]. At intermediate pH (pH 6.7), the shape of the spikes was not homogeneous and several forms of G could be observed [37]. In some regions, G seemed to have kept its high pH organization. Some spikes also had the typical post-fusion shape. Some elongated monomeric rod-like shape structures could be distinguished. The sequential appearance of the different species when lowering the pH suggested that the monomers were intermediates during the conformational change [37]. Indeed, independent refolding of monomers before re-association to form the post-fusion trimer overcomes some topological problems encountered if G remains trimeric all along the structural transition [39].

Structure of monomeric intermediates

For rhabdoviral glycoproteins, the existence of an equilibrium between their different conformations suggested that it could be possible to find appropriate conditions to trap intermediates and eventually crystallize them.

We were able to obtain several crystalline forms of CHAV G_{th}. The first one corresponded to the post-fusion conformation [14]. The comparison of this structure with that of VSV-G_{th} post-fusion conformation revealed that the PHD is the most divergent domain, with the largest differences confined to the secondary structure of the major antigenic site of rhabdoviruses glycoproteins. Local differences also indicated that CHAV has evolved alternative structural solutions in hinge regions between PHD and FD as well as distinct pH-sensitive switches [14].

More interestingly, the asymmetric unit of the second crystalline form contains four CHAV G_{th} molecules exhibiting two conformations distinct from those of VSV G_{th} pre-fusion and CHAV/VSV G_{th} post-fusion conformations [31] (Figs. 1b and 2). Those crystals were grown at pH 7.5, a pH at which VSV G_{th} was shown to assume a range of intermediate monomeric conformations in solution [37].

The first protomer conformation found in the crystal asymmetric unit corresponded to an early intermediate (CHAV G_{th} EI) on the transition pathway (Fig. 1b). This protomer looks like the protomer of VSV G pre-fusion state with a single, functionally major difference: the R5 segment has already left the hydrophobic groove it occupies in VSV G pre-fusion conformation [25,31].

The second protomer conformation corresponded to a late intermediate (CHAV G_{th} LI) on the transition pathway [24,31]. It is already in an elongated hairpin conformation. However, it is not superimposable with the protomer of CHAV G_{th} post-fusion state (Fig. 1b) due to incomplete refolding of R1, R4 and R5 [24,31].

Those two structures offer a plausible pathway for the conformational change (Fig. 1b) with three major features. The first is that R5 can leave the TrD groove it occupies in the pre-fusion conformation before any other structural change. This movement is likely triggered by protonation of a cluster of histidines (H60, H162, and H407) (Fig. 1b), destabilizing the FD-R5 interaction in the pre-fusion state of the protomer [25]. The second feature is that the central helix elongates in two stages; in the LI, the helix is longer than in the pre-fusion protomer but shorter than in the post-fusion one. The third feature

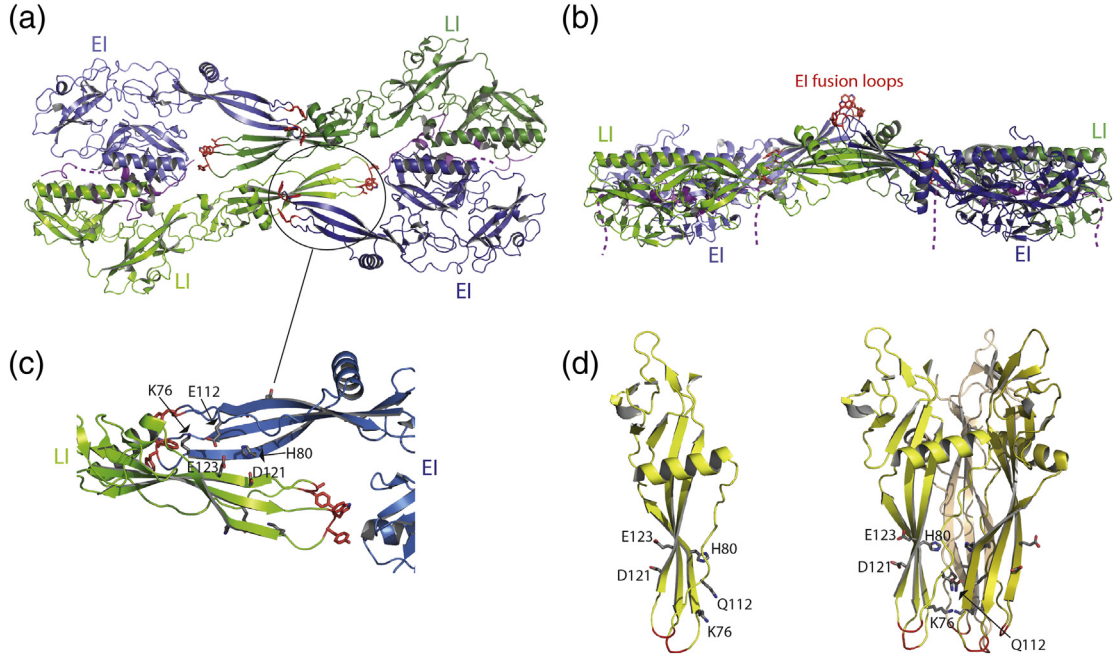

Fig. 2. Non-trimeric association of monomeric intermediate states of G. (a and b) Two views of the tetrameric assembly in the CHAV G_{th} crystal (PDB code: 5MDM) rotated by 90°. Protomers in the EI conformation are in blue. Protomers in the LI conformation are in green. The residues in the fusion loops at the tip of the FD are in red sticks. In panel B, the C-terminal segments which are linked to the transmembrane domain are depicted in dashed lines. (c) Close-up view of the antiparallel β-sheet formed between EI (in blue) and LI (in green) FDs in the crystal asymetric unit. Key residues which cluster at the interface are represented in gray sticks. The residues in the fusion loops at the tip of the FD are in red sticks. (d) Localization of residues K76, H80, Q112, D121, E123 in the FD in the pre-fusion protomer (left part) and trimeric post-fusion (right part) conformations of VSV G.

is that most of the structural transition occurs in a monomeric form and goes to an elongated hairpin-like conformation before trimerization. Therefore, in the case of rhabdovirus G, there is no need to postulate the existence of a trimeric pre-hairpin conformation resembling those proposed for class I and class II viral fusion glycoproteins.

An antiparallel interaction between FDs required for fusion

The orientational mobility of the CHAV G_{th} EI conformation, conferred by the release of the R5 segment from the groove it occupies in the pre-fusion conformation, allows EI to orientate its fusion loops toward the target membrane.

However, in the crystal asymmetric unit, CHAV G_{th} molecules assemble in a compact dimer of EI–LI heterodimers [31] (Fig. 2a and b). The tetramer thus formed is a flat structure, from which protrude the fusion loops of the two EI, with a thickness of about 50Å (Fig. 2b). The EI/LI dimers are stabilized by extensive contacts between hydrophobic residues of the central helix (Fig. 2a), and by positioning the R5 segment of one molecule in the hydrophobic groove of the TrD of the other. In turn, the EI/LI dimers assemble by associating their four FDs in an antiparallel arrangement (Fig. 2a and c) in which the two EI fusion loops are projected outside the tetramer (Fig. 2b). This arrangement is stabilized by the formation of an intermolecular β-sheet between two EI and LI FDs, involving residues 75 to 80 in the EI strand (located downstream of the first G fusion loop) and 120 to 125 in the LI strand (located downstream of the second fusion loop) (Fig. 2c).

In this region, two residues (D121, E123) were previously reported as sites of mutations affecting the fusion properties of both VSV [40,41] and viral hemorrhagic septicemia virus (VHSV, a fish rhabdovirus) [42], and a mutation in position 76 was shown to compensate for a deleterious mutation in the fusion loops [43]. The crystal structures of the pre- and post-fusion conformations did not provide a molecular explanation of those phenotypes (Fig. 2d). However, the fact that in the intermolecular β-sheet found in the new crystal form, residues in positions 121 and 123 on the LI side are facing the conserved H80 on the EI side, provides an explanation (Fig. 2c).

Indeed, it was shown further in VSV G that the H80A mutation, and the E123L and D121L double mutation, which both abolish VSV G fusion properties, were rescued by the same compensatory Q112P mutation. In a single FD, residue 112 is located on the opposite side of the three-stranded β-sheet and is far from residues 121 and 123 (Fig. 2d). However, in the CHAV G_{th} crystal structure, H80, E112, D121and E123 are clustered on the same side of the intermolecular β-sheet [31] (Fig. 2c). This strongly suggests that the antiparallel association of the FDs observed in the crystal of CHAV G_{th} is functionally relevant and crucial for fusion.

The antiparallel character of such an assembly implies that at this stage, the FDs are positioned parallel to the viral membrane (unlike their orthogonal orientation in pre- and post-fusion trimers).

Toward a model for vesiculovirus membrane fusion

Using an *in vitro* system to characterize fusion between VSV virions and liposomes, it has been demonstrated that the glycoproteins play two distinct roles (Fig. 3). First, in the contact zone with the target membrane, they drive the formation of the initial fusion pore (Fig. 3b and c). The flat base of the bullet-shaped virions is the favored site for this process [38]. We suggest that flat assemblies involving antiparallel interactions between the FD β-sheet, similar to those described in the previous paragraph, are involved at this stage. Such an assembly, by exposing the fusion loops, is ideally suited to constitute the first bridge between the target membrane and the flat base of the viral particle (Fig. 3b). Several features should favor the formation of such intermediates specifically at the flat base of the virus, including the difference in membrane curvature (which is zero at the viral base), the lower density of viral glycoproteins [38] and maybe also distinct interactions with intraviral matrix proteins which may control G oligomeric status. Whether several such dimer-based assemblies cooperate to initiate the fusion process remains an open question. In addition, the fate of those oligomers at later stages of the fusion process is unknown.

The second stage is pore enlargement (Fig. 3d), which is the most energetically expensive step [44]. It has been shown that the spikes located outside the contact zone play a decisive role in this ultimate step by forming a helical network of post-fusion trimers [38]. Here, the structural transition toward the post-fusion trimer proceeds through monomeric EI and LI conformations (Fig. 3).

It is worth noting that, using native mass spectrometry, dimeric assemblies of both VSV G and CHAV G have been detected at pH 7.5 [31]. At such a pH, post-fusion trimers are not yet formed. Together with the progressive pH decrease after virion endocytosis, this might allow a for temporal regulation of the formation of the different oligomeric species.

Differences and similarities with other viral fusion glycoproteins

We are aware that our structural data challenge the current model proposed for both class I and

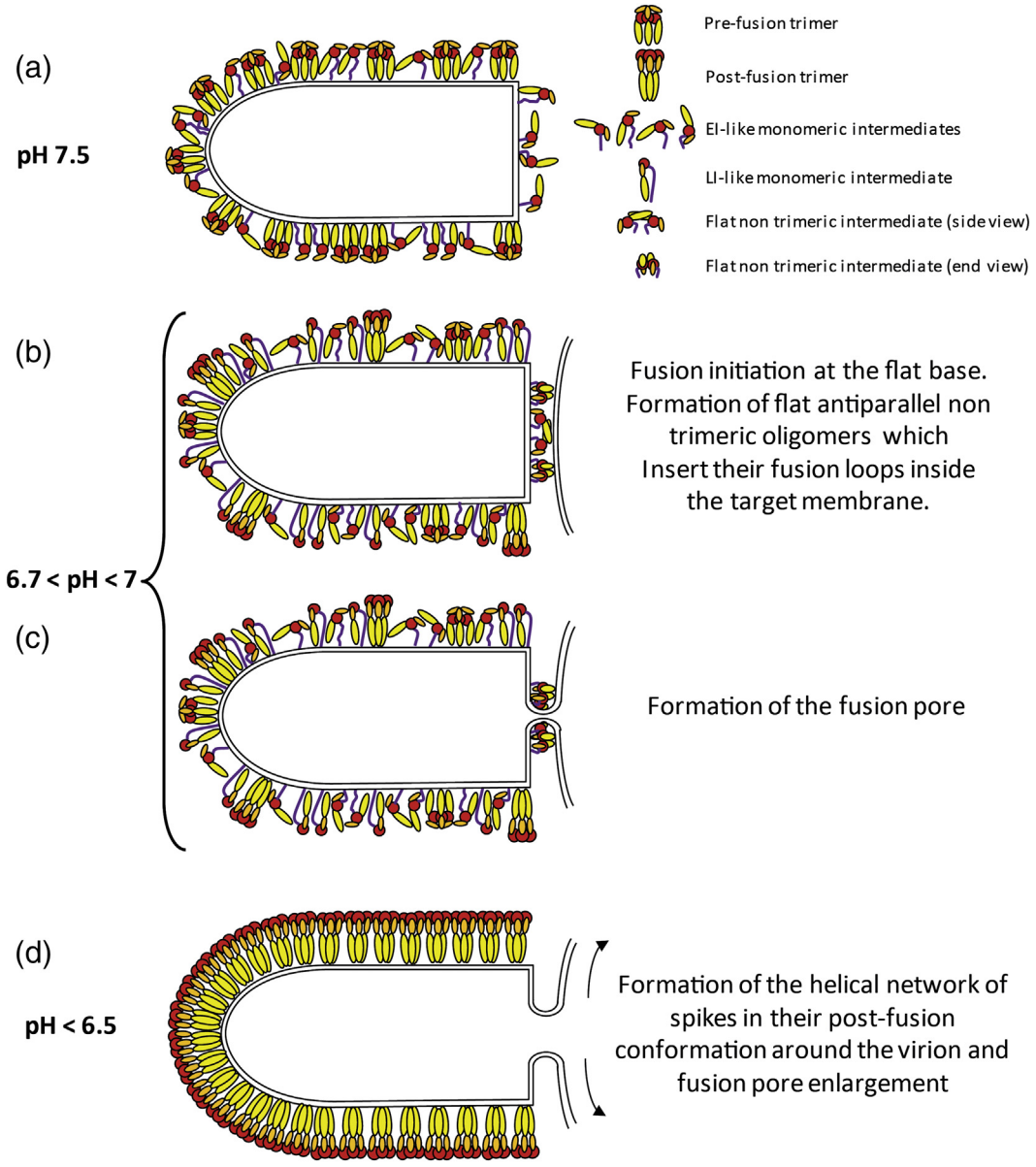

Fig. 3. A model for VSV membrane fusion. (a) At pH 7.5 in the absence of a target membrane, at the viral surface, there is an equilibrium between G pre-fusion trimer and flexible monomers [37,38] mostly in an EI-like conformation having different orientations, thanks to the flexibility of the R5 segment [31]. (b) Lowering the pH below 7 progressively shifts the equilibrium toward more elongated monomers in an LI-like conformation [31,37]. Some post-fusion trimers are already present on the lateral side of the virus. The flat base is a favorable site for the association of monomeric intermediates into flat antiparallel dimers, which insert their fusion loops in the target membrane. (c) Formation of the fusion pore. The number of oligomers involved at this stage and their exact organization around the fusion pore is not known. For convenience, on the scheme, the fusion pore has been placed at the center of the flat base. However, note that the membrane is strongly constrained at the edge of the base, a feature that might favor pore formation at this location. (d) The formation of the helical network of spikes in their post-fusion conformation on the lateral side of the virion drives the enlargement of the initial fusion pore leading to complete membrane merger. What happens to the dimers that were involved in the initiation of the fusion process is unknown. The simplest explanation is that the dimeric association is only transient and that the dimer dissociates upon protomers refolding to LI and final retrimerization.

class II fusion glycoproteins [16], and sometimes for class III glycoproteins [26,27]. The current model postulates the formation of the so-called trimeric elongated pre-hairpin conformation that bridges the viral and target membranes. For class I [45–48] and class II [49–51], several experimental data are consistent with this model. However, the pathway of the structural transition that we propose for vesiculovirus

G does not go through such a trimeric elongated pre-hairpin conformation, which has never been observed at the viral surface.

The question, which then arises, is whether the working of the vesiculovirus machinery is different from that of other viruses. This is all the more pertinent because (i) all the experimental data suggest that the membrane fusion pathway (i.e., the lipidic intermediates which are formed) is very similar for all the enveloped viruses studied so far regardless of the organization of their fusion machinery [52–54], and (ii) fusion kinetics of individual virions for influenza virus (class I), West Nile virus (class II), and VSV could all be fit to models based on very similar sequence of conformational events [13,55,56]. Therefore, in this last part, we will discuss data obtained on other viral fusion glycoproteins from both class I and class II and focus on some features reminiscent of what is observed for vesiculovirus G.

First, class II fusion proteins are known to transition from a (homo- or hetero-) pre-fusion dimer to a post-fusion trimer [57–62] through a monomeric intermediate [63,64], and a crystalline structure of a monomer of Rift Valley fever virus (a phlebovirus, member of the bunyaviridae family) Gc in an extended conformation, which may represent a transition intermediate, has been determined [65]. Indeed, several experiments have indicated that class II fusion glycoproteins are monomeric when they interact with the target membrane [66]. Cryo-electron tomography (cryo-ET) analysis revealed bridge-like densities between acidified virions and liposomes with dimensions consistent with those of extended monomers for Rift Valley fever virus [67], Uukuniemi virus (another phlebovirus) [68] and Sindbis virus (an alphavirus) [69]. In the latter case, the orientation of the fusion glycoprotein (E1) relative to the virus surface appeared to be variable. The bridge-like densities between the virus and target membrane were either normal or at a slant relative to the virus surface. As suggested by the authors, this flexibility might allow E1 to bind the target membrane at different distances and curvatures [69]. The stage of the refolding process at which trimerization occurs still remains a matter of debate. Indeed, different conclusions have been drawn depending on the virus and the experiments. Biochemical data have suggested that, for Semliki Forest virus (an alphavirus) and Dengue virus (a flavivirus), trimer formation is relatively rapid and precedes the folding back of the carboxy-terminal domain [49–51]. On the other hand, for tick-borne encephalitis virus (a flavivirus), it has been suggested that trimerization may occur at a late stage of the refolding process [66].

Second, in the case of class I fusion glycoproteins, which are trimeric in both their pre- and post-fusion states [16], it is well known that their ectodomains are often monomeric when expressed in the absence of the transmembrane domain. To obtain a stable trimeric pre-fusion structure, the C-terminal part of the ectodomain is fused to a trimerization motif, based either on the transcription factor GCN4, as in the case of coronavirus S [70], parainfluenza virus 5 F glycoproteins [71] and Hendra virus F glycoprotein [72], or the T4 fibritin motif, as in the case of respiratory syncytial virus fusion glycoprotein [73]. Even for influenza HA, the dogma of the stability of the trimeric state all along the structural transition could be called into question in view of the growing number of crystalline structures that do not display any threefold symmetry (PDB entry codes: 4EDA, 5A3I 5K9K, 5K9O and 5IBL) [74–77] (Fig. 4). More remarkably, in those crystal structures, the monomer structure is quite different from the structure of HA protomer in the trimeric pre-fusion state (Fig. 4b). Particularly, the helix A is longer as part of the loop has initiated its transition toward a helical conformation (Fig. 4b). On the other hand, the helix B is shorter (Fig. 4b). The fact that several crystalline structures of distinct HA subtypes contain a monomeric conformation suggests that it cannot be only a crystallization artifact and that those monomers might be transient intermediates that are trapped during the crystallization process. All those monomeric structures have been obtained in complex with a Fab, which may also have contributed to their catching in the crystal. If those structures correspond to real intermediates, they suggest a refolding pathway for HA monomer in which helix A elongation progressively displaces the loop in the structure of the helix B until this loop reaches the position it occupies in the post-fusion structure of HA2.

It is worth noting that EM images and cryo-ET have also provided several views of the membrane remodeling events and some structural snapshots of HA during the fusion process [81–84]. They are consistent with the initial formation of flexible extended intermediates which interact with the target membrane and refold into a post-fusion-like structure which is perpendicular to the axis of the fusion pore (i.e., parallel to the fusing membranes). However, the resolution of those structures is not sufficient to definitively conclude on their oligomeric state, although the authors suggest that they might be trimeric [84].

Finally, the formation of a regular network of fusion glycoproteins in their post-fusion state is not exclusive of vesiculovirus G. More or less regular networks have been also observed with other class III fusion glycoproteins such as pseudorabies gB [85] and several class II fusion glycoproteins [51,86,87]. As suggested for vesiculoviruses [38], it is possible that the glycoproteins located outside the contact zone between fusing membranes have a role, probably at a late stage of the fusion process (i.e., enlargement of the fusion pore) via the formation of more or less regular arrays.

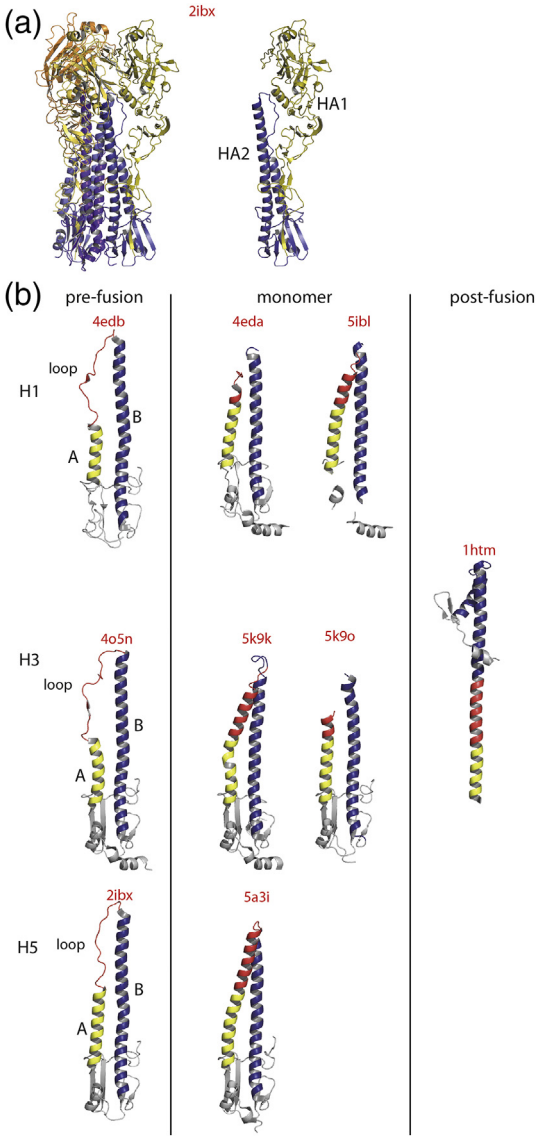

Fig. 4. Monomeric HA structures. (a) Structure of HA pre-fusion state (H5 subtype, PDB code 2IBX [78]). Left: Ribbon diagram of HA pre-fusion trimer. The HA1 subunits are colored in a shade of yellow. The HA2 subunits are colored in a shade of blue. Right: Ribbon diagram of HA protomer. (b) First row: ribbon diagrams of HA2 structure (H1 subtype) as in the pre-fusion protomer [74] and in two monomeric HA structures [74,77]. Second row: ribbon diagrams of HA2 structure (H3 subtype) [79] as in the pre-fusion protomer, in two monomeric HA0 structures [76] and as in its trimeric post-fusion conformation [80]. Third row: ribbon diagrams of HA2 structure (H5 subtype) as in the pre-fusion protomer [78] and in a monomeric HA structures [75]. The residues are colored by their secondary structure in the pre-fusion protomer. Residues corresponding to helix A are in yellow, to helix B in blue and to the loop located between helices A and B in red. In several monomers, the part of the chain corresponding to the loop between helices A and B is not visible in the crystal. All the structures are aligned on helix A of the prefusion protomer. The corresponding PDB codes are indicated above each structure.

Final remarks and conclusion

The determination of an increasing number of structures of viral fusion and the associated functional studies have shed light on the working of the fusion machinery. Globally, this has revealed similar principles of action even if the proteins involved have very different structural organizations. However, the nature of intermediates and how they cooperate inside and potentially outside the target membrane contact zone remain largely elusive.

Novel structures of such intermediates are required to complete our understanding of the transition pathway for each class of viral fusion glycoproteins. Cryo-EM and cryo-ET enhanced by direct electron detection devices, improved microscopes with more stable optics, and advances in image processing software [88–91] should make it possible to visualize the conformation of the glycoproteins while they interact with a target membrane. Indeed, as mentioned above, some progresses have already been made for both class I [81–84,92] and class II fusion glycoproteins [67–69]; however, a higher resolution will be required to get a reliable quasi-atomic model of those intermediates.

Acknowledgments

We thank Nathan Jespersen for providing language help and careful reading of the manuscript. This work was supported by a grant from ANR (ANR CE11 MOBARHE) to Y.G.

Received 31 January 2018;
Received in revised form 6 April 2018;
Accepted 10 April 2018
Available online 18 April 2018

Keywords:
Vesiculovirus;
Influenza;
glycoprotein;
membrane fusion;
conformational change

Abbreviations used:
VSV, vesicular stomatitis virus; CHAV, Chandipura virus; G, glycoprotein; HA, hemagglutinin; EM, electron microscopy; FD, fusion domain; PHD, pleckstrin homology domain; TrD, trimerization domain; PDB, Protein Data Bank; cryo-ET, cryo-electron tomography.

References

[1] G.N. Barber, Vsv-tumor selective replication and protein translation, Oncogene 24 (2005) 7710–7719.

[2] M. Fernandez, M. Porosnicu, D. Markovic, G.N. Barber, Genetically engineered vesicular stomatitis virus in gene therapy: application for treatment of malignant disease, J. Virol. 76 (2002) 895–904.
[3] E. Hastie, V.Z. Grdzelishvili, Vesicular stomatitis virus as a flexible platform for oncolytic virotherapy against cancer, J. Gen. Virol. 93 (2012) 2529–2545.
[4] S. Menghani, R. Chikhale, A. Raval, P. Wadibhasme, P. Khedekar, Chandipura virus: an emerging tropical pathogen, Acta Trop. 124 (2012) 1–14.
[5] A.A.V. Albertini, E. Baquero, A. Ferlin, Y. Gaudin, Molecular and cellular aspects of rhabdovirus entry, Viruses 4 (2012) 117–139.
[6] D. Finkelshtein, A. Werman, D. Novick, S. Barak, M. Rubinstein, Ldl receptor and its family members serve as the cellular receptors for vesicular stomatitis virus, Proc. Natl. Acad. Sci. U. S. A. 110 (2013) 7306–7311.
[7] J. Nikolic, L. Belot, H. Raux, P. Legrand, Y. Gaudin, A.A. Albertini, Structural basis for the recognition of ldl-receptor family members by vsv glycoprotein, Nat. Commun. 9 (2018) 1029.
[8] D.K. Cureton, R.H. Massol, S. Saffarian, T.L. Kirchhausen, S. P. Whelan, Vesicular stomatitis virus enters cells through vesicles incompletely coated with clathrin that depend upon actin for internalization, PLoS Pathog. 5 (2009), e1000394.
[9] H.K. Johannsdottir, R. Mancini, J. Kartenbeck, L. Amato, A. Helenius, Host cell factors and functions involved in vesicular stomatitis virus entry, J. Virol. 83 (2009) 440–453.
[10] S. Roche, A.A. Albertini, J. Lepault, S. Bressanelli, Y. Gaudin, Structures of vesicular stomatitis virus glycoprotein: membrane fusion revisited, Cell. Mol. Life Sci. 65 (2008) 1716–1728.
[11] R.W. Doms, D.S. Keller, A. Helenius, W.E. Balch, Role for adenosine triphosphate in regulating the assembly and transport of vesicular stomatitis virus g protein trimers, J. Cell Biol. 105 (1987) 1957–1969.
[12] Y. Gaudin, C. Tuffereau, D. Segretain, M. Knossow, A. Flamand, Reversible conformational changes and fusion activity of rabies virus glycoprotein, J. Virol. 65 (1991) 4853–4859.
[13] I.S. Kim, S. Jenni, M.L. Stanifer, E. Roth, S.P. Whelan, A.M. van Oijen, S.C. Harrison, Mechanism of membrane fusion induced by vesicular stomatitis virus g protein, Proc. Natl. Acad. Sci. U. S. A. 114 (2017) E28–E36.
[14] E. Baquero, A.A. Albertini, H. Raux, L. Buonocore, J.K. Rose, S. Bressanelli, Y. Gaudin, Structure of the low pH conformation of chandipura virus g reveals important features in the evolution of the vesiculovirus glycoprotein, PLoS Pathog. 11 (2015), e1004756.
[15] S. Roche, Y. Gaudin, Characterization of the equilibrium between the native and fusion-inactive conformation of rabies virus glycoprotein indicates that the fusion complex is made of several trimers, Virology 297 (2002) 128–135.
[16] S.C. Harrison, Viral membrane fusion, Virology 479-480 (2015) 498–507.
[17] J. Kadlec, S. Loureiro, N.G. Abrescia, D.I. Stuart, I.M. Jones, The postfusion structure of baculovirus gp64 supports a unified view of viral fusion machines, Nat. Struct. Mol. Biol. 15 (2008) 1024–1030.
[18] M. Backovic, R. Longnecker, T.S. Jardetzky, Structure of a trimeric variant of the Epstein–Barr virus glycoprotein b, Proc. Natl. Acad. Sci. U. S. A. 106 (2009) 2880–2885.
[19] H.G. Burke, E.E. Heldwein, Crystal structure of the human cytomegalovirus glycoprotein b, PLoS Pathog. 11 (2015), e1005227.
[20] S. Chandramouli, C. Ciferri, P.A. Nikitin, S. Calo, R. Gerrein, K. Balabanis, J. Monroe, C. Hebner, A.E. Lilja, E.C. Settembre, et al., Structure of hcmv glycoprotein b in the postfusion conformation bound to a neutralizing human antibody, Nat. Commun. 6 (2015) 8176.
[21] E.E. Heldwein, H. Lou, F.C. Bender, G.H. Cohen, R.J. Eisenberg, S.C. Harrison, Crystal structure of glycoprotein b from herpes simplex virus 1, Science 313 (2006) 217–220.
[22] R. Peng, S. Zhang, Y. Cui, Y. Shi, G.F. Gao, J. Qi, Structures of human-infecting thogotovirus fusogens support a common ancestor with insect baculovirus, Proc. Natl. Acad. Sci. U. S. A. 114 (2017) E8905–E8912.
[23] E. Baquero, A.A. Albertini, Y. Gaudin, Recent mechanistic and structural insights on class III viral fusion glycoproteins, Curr. Opin. Struct. Biol. 33 (2015) 52–60.
[24] S. Roche, S. Bressanelli, F.A. Rey, Y. Gaudin, Crystal structure of the low-pH form of the vesicular stomatitis virus glycoprotein g, Science 313 (2006) 187–191.
[25] S. Roche, F.A. Rey, Y. Gaudin, S. Bressanelli, Structure of the prefusion form of the vesicular stomatitis virus glycoprotein g, Science 315 (2007) 843–848.
[26] J. Fontana, D. Atanasiu, W.T. Saw, J.R. Gallagher, R.G. Cox, J. C. Whitbeck, L.M. Brown, R.J. Eisenberg, G.H. Cohen, The fusion loops of the initial prefusion conformation of herpes simplex virus 1 fusion protein point toward the membrane, MBio 8 (2017).
[27] T. Zeev-Ben-Mordehai, D. Vasishtan, A. Hernandez Duran, B. Vollmer, P. White, A. Prasad Pandurangan, C.A. Siebert, M. Topf, K. Grunewald, Two distinct trimeric conformations of natively membrane-anchored full-length herpes simplex virus 1 glycoprotein b, Proc. Natl. Acad. Sci. U. S. A. 113 (2016) 4176–4181.
[28] J.R. Gallagher, D. Atanasiu, W.T. Saw, M.J. Paradisgarten, J.C. Whitbeck, R.J. Eisenberg, G.H. Cohen, Functional fluorescent protein insertions in herpes simplex virus gb report on gb conformation before and after execution of membrane fusion, PLoS Pathog. 10 (2014), e1004373.
[29] W. Weissenhorn, A. Carfi, K.H. Lee, J.J. Skehel, D.C. Wiley, Crystal structure of the ebola virus membrane fusion subunit, gp2, from the envelope glycoprotein ectodomain, Mol. Cell 2 (1998) 605–616.
[30] W. Weissenhorn, A. Dessen, S.C. Harrison, J.J. Skehel, D.C. Wiley, Atomic structure of the ectodomain from HIV-1 gp41, Nature 387 (1997) 426–430.
[31] E. Baquero, A.A. Albertini, H. Raux, A. Abou-Hamdan, E. Boeri-Erba, M. Ouldali, L. Buonocore, J.K. Rose, J. Lepault, S. Bressanelli, et al., Structural intermediates in the fusion-associated transition of vesiculovirus glycoprotein, EMBO J. 36 (2017) 679–692.
[32] D.L. Crimmins, W.B. Mehard, S. Schlesinger, Physical properties of a soluble form of the glycoprotein of vesicular stomatitis virus at neutral and acidic pH, Biochemistry 22 (1983) 5790–5796.
[33] D.S. Lyles, V.A. Varela, J.W. Parce, Dynamic nature of the quaternary structure of the vesicular stomatitis virus envelope glycoprotein, Biochemistry 29 (1990) 2442–2449.
[34] P. Zagouras, J.K. Rose, Dynamic equilibrium between vesicular stomatitis virus glycoprotein monomers and trimers in the Golgi and at the cell surface, J. Virol. 67 (1993) 7533–7538.
[35] P. Zagouras, A. Ruusala, J.K. Rose, Dissociation and reassociation of oligomeric viral glycoprotein subunits in the endoplasmic reticulum, J. Virol. 65 (1991) 1976–1984.
[36] I.A. Wilson, J.J. Skehel, D.C. Wiley, Structure of the haemagglutinin membrane glycoprotein of influenza virus at 3 a resolution, Nature 289 (1981) 366–373.

[37] A.A. Albertini, C. Merigoux, S. Libersou, K. Madiona, S. Bressanelli, S. Roche, J. Lepault, R. Melki, P. Vachette, Y. Gaudin, Characterization of monomeric intermediates during vsv glycoprotein structural transition, PLoS Pathog. 8 (2012), e1002556.
[38] S. Libersou, A.A. Albertini, M. Ouldali, V. Maury, C. Maheu, H. Raux, F. de Haas, S. Roche, Y. Gaudin, J. Lepault, Distinct structural rearrangements of the vsv glycoprotein drive membrane fusion, J. Cell Biol. 191 (2010) 199–210.
[39] E. Baquero, A.A. Albertini, P. Vachette, J. Lepault, S. Bressanelli, Y. Gaudin, Intermediate conformations during viral fusion glycoprotein structural transition, Curr. Opin. Virol. 3 (2013) 143–150.
[40] B.L. Fredericksen, M.A. Whitt, Mutations at two conserved acidic amino acids in the glycoprotein of vesicular stomatitis virus affect pH-dependent conformational changes and reduce the pH threshold for membrane fusion, Virology 217 (1996) 49–57.
[41] L. Zhang, H.P. Ghosh, Characterization of the putative fusogenic domain in vesicular stomatitis virus glycoprotein g, J. Virol. 68 (1994) 2186–2193.
[42] Y. Gaudin, P. de Kinkelin, A. Benmansour, Mutations in the glycoprotein of viral haemorrhagic septicaemia virus that affect virulence for fish and the pH threshold for membrane fusion, J. Gen. Virol. 80 (1999) 1221–1229.
[43] M.L. Stanifer, D.K. Cureton, S.P. Whelan, A recombinant vesicular stomatitis virus bearing a lethal mutation in the glycoprotein gene uncovers a second site suppressor that restores fusion, J. Virol. 85 (2011) 8105–8115.
[44] F.S. Cohen, G.B. Melikyan, The energetics of membrane fusion from binding, through hemifusion, pore formation, and pore enlargement, J. Membr. Biol. 199 (2004) 1–14.
[45] R.A. Furuta, C.T. Wild, Y. Weng, C.D. Weiss, Capture of an early fusion-active conformation of hiv-1 gp41, Nat. Struct. Biol. 5 (1998) 276–279.
[46] Y.H. Kim, J.E. Donald, G. Grigoryan, G.P. Leser, A.Y. Fadeev, R.A. Lamb, W.F. DeGrado, Capture and imaging of a prehairpin fusion intermediate of the paramyxovirus piv5, Proc. Natl. Acad. Sci. U. S. A. 108 (2011) 20992–20997.
[47] C.J. Russell, T.S. Jardetzky, R.A. Lamb, Membrane fusion machines of paramyxoviruses: capture of intermediates of fusion, EMBO J. 20 (2001) 4024–4034.
[48] C.T. Wild, D.C. Shugars, T.K. Greenwell, C.B. McDanal, T.J. Matthews, Peptides corresponding to a predictive alpha-helical domain of human immunodeficiency virus type 1 gp41 are potent inhibitors of virus infection, Proc. Natl. Acad. Sci. U. S. A. 91 (1994) 9770–9774.
[49] M. Liao, M. Kielian, Domain III from class II fusion proteins functions as a dominant-negative inhibitor of virus membrane fusion, J. Cell Biol. 171 (2005) 111–120.
[50] G. Roman-Sosa, M. Kielian, The interaction of alphavirus e1 protein with exogenous domain III defines stages in virus-membrane fusion, J. Virol. 85 (2011) 12271–12279.
[51] C. Sanchez-San Martin, H. Sosa, M. Kielian, A stable prefusion intermediate of the alphavirus fusion protein reveals critical features of class II membrane fusion, Cell Host Microbe 4 (2008) 600–608.
[52] L.V. Chernomordik, V.A. Frolov, E. Leikina, P. Bronk, J. Zimmerberg, The pathway of membrane fusion catalyzed by influenza hemagglutinin: restriction of lipids, hemifusion, and lipidic fusion pore formation, J. Cell Biol. 140 (1998) 1369–1382.
[53] Y. Gaudin, Rabies virus-induced membrane fusion pathway, J. Cell Biol. 150 (2000) 601–612.
[54] E. Zaitseva, A. Mittal, D.E. Griffin, L.V. Chernomordik, Class II fusion protein of alphaviruses drives membrane fusion through the same pathway as class i proteins, J. Cell Biol. 169 (2005) 167–177.
[55] L.H. Chao, D.E. Klein, A.G. Schmidt, J.M. Pena, S.C. Harrison, Sequential conformational rearrangements in flavivirus membrane fusion, elife 3 (2014), e04389.
[56] T. Ivanovic, J.L. Choi, S.P. Whelan, A.M. van Oijen, S.C. Harrison, Influenza-virus membrane fusion by cooperative fold-back of stochastically induced hemagglutinin intermediates, elife 2 (2013), e00333.
[57] S. Bressanelli, K. Stiasny, S.L. Allison, E.A. Stura, S. Duquerroy, J. Lescar, F.X. Heinz, F.A. Rey, Structure of a flavivirus envelope glycoprotein in its low-pH-induced membrane fusion conformation, EMBO J. 23 (2004) 728–738.
[58] D.L. Gibbons, M.C. Vaney, A. Roussel, A. Vigouroux, B. Reilly, J. Lepault, M. Kielian, F.A. Rey, Conformational change and protein-protein interactions of the fusion protein of semliki forest virus, Nature 427 (2004) 320–325.
[59] J. Lescar, A. Roussel, M.W. Wien, J. Navaza, S.D. Fuller, G. Wengler, G. Wengler, F.A. Rey, The fusion glycoprotein shell of semliki forest virus: an icosahedral assembly primed for fusogenic activation at endosomal pH, Cell 105 (2001) 137–148.
[60] Y. Modis, S. Ogata, D. Clements, S.C. Harrison, A ligand-binding pocket in the dengue virus envelope glycoprotein, Proc. Natl. Acad. Sci. U. S. A. 100 (2003) 6986–6991.
[61] Y. Modis, S. Ogata, D. Clements, S.C. Harrison, Structure of the dengue virus envelope protein after membrane fusion, Nature 427 (2004) 313–319.
[62] F.A. Rey, F.X. Heinz, C. Mandl, C. Kunz, S.C. Harrison, The envelope glycoprotein from tick-borne encephalitis virus at 2 Å resolution, Nature 375 (1995) 291–298.
[63] K. Stiasny, S.L. Allison, A. Marchler-Bauer, C. Kunz, F.X. Heinz, Structural requirements for low-pH-induced rearrangements in the envelope glycoprotein of tick-borne encephalitis virus, J. Virol. 70 (1996) 8142–8147.
[64] J.M. Wahlberg, H. Garoff, Membrane fusion process of semliki forest virus. I: low pH-induced rearrangement in spike protein quaternary structure precedes virus penetration into cells, J. Cell Biol. 116 (1992) 339–348.
[65] M. Dessau, Y. Modis, Crystal structure of glycoprotein c from rift valley fever virus, Proc. Natl. Acad. Sci. U. S. A. 110 (2013) 1696–1701.
[66] K. Stiasny, C. Kossl, J. Lepault, F.A. Rey, F.X. Heinz, Characterization of a structural intermediate of flavivirus membrane fusion, PLoS Pathog. 3 (2007), e20.
[67] S. Halldorsson, S. Li, M. Li, K. Harlos, T.A. Bowden, J.T. Huiskonen, Shielding and activation of a viral membrane fusion protein, Nat. Commun. 9 (2018) 349.
[68] D. Bitto, S. Halldorsson, A. Caputo, J.T. Huiskonen, Low pH and anionic lipid-dependent fusion of uukuniemi pHlebovirus to liposomes, J. Biol. Chem. 291 (2016) 6412–6422.
[69] S. Cao, W. Zhang, Characterization of an early-stage fusion intermediate of sindbis virus using cryoelectron microscopy, Proc. Natl. Acad. Sci. U. S. A. 110 (2013) 13362–13367.
[70] A. Walls, M.A. Tortorici, B.J. Bosch, B. Frenz, P.J. Rottier, F. DiMaio, F.A. Rey, D. Veesler, Crucial steps in the structure determination of a coronavirus spike glycoprotein using cryo-electron microscopy, Protein Sci. 26 (2017) 113–121.
[71] H.S. Yin, X. Wen, R.G. Paterson, R.A. Lamb, T.S. Jardetzky, Structure of the parainfluenza virus 5 f protein in its metastable, prefusion conformation, Nature 439 (2006) 38–44.

[72] J.J. Wong, R.G. Paterson, R.A. Lamb, T.S. Jardetzky, Structure and stabilization of the hendra virus f glycoprotein in its prefusion form, Proc. Natl. Acad. Sci. U. S. A. 113 (2016) 1056–1061.
[73] J.S. McLellan, M. Chen, S. Leung, K.W. Graepel, X. Du, Y. Yang, T. Zhou, U. Baxa, E. Yasuda, T. Beaumont, et al., Structure of rsv fusion glycoprotein trimer bound to a prefusion-specific neutralizing antibody, Science 340 (2013) 1113–1117.
[74] K.J. Cho, J.H. Lee, K.W. Hong, S.H. Kim, Y. Park, J.Y. Lee, S. Kang, S. Kim, J.H. Yang, E.K. Kim, et al., Insight into structural diversity of influenza virus haemagglutinin, J. Gen. Virol. 94 (2013) 1712–1722.
[75] X. Xiong, D. Corti, J. Liu, D. Pinna, M. Foglierini, L.J. Calder, S. R. Martin, Y.P. Lin, P.A. Walker, P.J. Collins, et al., Structures of complexes formed by h5 influenza hemagglutinin with a potent broadly neutralizing human monoclonal antibody, Proc. Natl. Acad. Sci. U. S. A. 112 (2015) 9430–9435.
[76] M.G. Joyce, A.K. Wheatley, P.V. Thomas, G.Y. Chuang, C. Soto, R.T. Bailer, A. Druz, I.S. Georgiev, R.A. Gillespie, M. Kanekiyo, et al., Vaccine-induced antibodies that neutralize group 1 and group 2 influenza a viruses, Cell 166 (2016) 609–623.
[77] D.D. Raymond, S.M. Stewart, J. Lee, J. Ferdman, G. Bajic, K. T. Do, M.J. Ernandes, P. Suphaphiphat, E.C. Settembre, P. R. Dormitzer, et al., Influenza immunization elicits antibodies specific for an egg-adapted vaccine strain, Nat. Med. 22 (2016) 1465–1469.
[78] S. Yamada, Y. Suzuki, T. Suzuki, M.Q. Le, C.A. Nidom, Y. Sakai-Tagawa, Y. Muramoto, M. Ito, M. Kiso, T. Horimoto, et al., Haemagglutinin mutations responsible for the binding of H5N1 influenza a viruses to human-type receptors, Nature 444 (2006) 378–382.
[79] P.S. Lee, N. Ohshima, R.L. Stanfield, W. Yu, Y. Iba, Y. Okuno, Y. Kurosawa, I.A. Wilson, Receptor mimicry by antibody F045-092 facilitates universal binding to the H3 subtype of influenza virus, Nat. Commun. 5 (2014) 3614.
[80] P.A. Bullough, F.M. Hughson, J.J. Skehel, D.C. Wiley, Structure of influenza haemagglutinin at the pH of membrane fusion, Nature 371 (1994) 37–43.
[81] K.K. Lee, Architecture of a nascent viral fusion pore, EMBO J. 29 (2010) 1299–1311.
[82] P. Chlanda, E. Mekhedov, H. Waters, C.L. Schwartz, E.R. Fischer, R.J. Ryham, F.S. Cohen, P.S. Blank, J. Zimmerberg, The hemifusion structure induced by influenza virus haemagglutinin is determined by physical properties of the target membranes, Nat. Microbiol. 1 (2016), 16050.
[83] L. Gui, J.L. Ebner, A. Mileant, J.A. Williams, K.K. Lee, Visualization and sequencing of membrane remodeling leading to influenza virus fusion, J. Virol. 90 (2016) 6948–6962.
[84] L.J. Calder, P.B. Rosenthal, Cryomicroscopy provides structural snapshots of influenza virus membrane fusion, Nat. Struct. Mol. Biol. 23 (2016) 853–858.
[85] M. Vallbracht, D. Brun, M. Tassinari, M.C. Vaney, G. Pehau-Arnaudet, P. Guardado-Calvo, A. Haouz, B.G. Klupp, T.C. Mettenleiter, F.A. Rey, et al., Structure-function dissection of the pseudorabies virus glycoprotein b fusion loops, J. Virol. 92 (2018) e01203–e01217.
[86] D.L. Gibbons, I. Erk, B. Reilly, J. Navaza, M. Kielian, F.A. Rey, J. Lepault, Visualization of the target-membrane-inserted fusion protein of semliki forest virus by combined electron microscopy and crystallography, Cell 114 (2003) 573–583.
[87] K. Stiasny, S. Bressanelli, J. Lepault, F.A. Rey, F.X. Heinz, Characterization of a membrane-associated trimeric low-pH-induced form of the class II viral fusion protein e from tick-borne encephalitis virus and its crystallization, J. Virol. 78 (2004) 3178–3183.
[88] L.A. Baker, M. Grange, K. Grunewald, Electron cryo-tomography captures macromolecular complexes in native environments, Curr. Opin. Struct. Biol. 46 (2017) 149–156.
[89] C.K. Cassidy, B.A. Himes, Z. Luthey-Schulten, P. Zhang, Cryoem-based hybrid modeling approaches for structure determination, Curr. Opin. Microbiol. 43 (2017) 14–23.
[90] D. Elmlund, S.N. Le, H. Elmlund, High-resolution cryo-em: the nuts and bolts, Curr. Opin. Struct. Biol. 46 (2017) 1–6.
[91] K.R. Vinothkumar, R. Henderson, Single particle electron cryomicroscopy: trends, issues and future perspective, Q. Rev. Biophys. 49 (2016), e13.
[92] G. Cardone, M. Brecher, J. Fontana, D.C. Winkler, C. Butan, J.M. White, A.C. Steven, Visualization of the two-step fusion process of the retrovirus avian sarcoma/leukosis virus by cryo-electron tomography, J. Virol. 86 (2012) 12129–12137.